Title	Relaxation and diffusion in a globally coupled Hamiltonian system
Author(s)	Yamaguchi, Yoshiyuki Y.
Citation	PHYSICAL REVIEW E (2003), 68(6)
Issue Date	2003-12-30
URL	http://hdl.handle.net/2433/53453
Right	Copyright 2003 American Physical Society
Type	Journal Article
Textversion	publisher

Relaxation and diffusion in a globally coupled Hamiltonian system

Yoshiyuki Y. Yamaguchi*
Department of Applied Mathematics and Physics, Kyoto University, Kyoto 606-8501, Japan
and Dipartimento di Energetica, Università degli Studi di Firenze, Via Santa Marta 3, I-50139 Firenze, Italy
(Received 13 September 2002; revised manuscript received 20 June 2003; published 30 December 2003)

The relation between relaxation and diffusion is investigated in a Hamiltonian system of globally coupled rotators. Diffusion is anomalous if and only if the system is going towards equilibrium. The anomaly in diffusion is not anomalous diffusion taking a power-type function, but is a transient anomaly due to nonstationarity. For a certain type of initial condition, in quasistationary states, diffusion can be explained by a stretched exponential correlation function, whose stretching exponent is almost constant and correlation time is linear as functions of degrees of freedom. The full time evolution is characterized by varying stretching exponent and correlation time.

DOI: 10.1103/PhysRevE.68.066210 PACS number(s): 05.45.Pq, 05.20.−y, 05.60.Cd, 05.70.Fh

I. INTRODUCTION

Relaxation to thermal equilibrium has been studied in Hamiltonian systems with long-range interactions [1–6]. One of the characteristic phenomena in the relaxation process is anomalous diffusion, since normal diffusion is expected at equilibrium. Anomalous diffusion was first investigated in a one-dimensional chaotic map to describe enhanced diffusion in Josephson junctions [7], and is observed in many systems both numerically [3,8–11] and experimentally [12].

Anomalous diffusion is also observed in Hamiltonian dynamical systems. It is explained as due to power-type distribution functions [8,13,14] of trapping and untrapping times of the orbit in the self-similar hierarchy of cylindrical cantori [15]. Self-similarity is expected to be one of the important concepts to understand statistics and motion in Hamiltonian systems, but cannot be the main feature in systems with many degrees of freedom. Then, as the first step of approaching the study of self-similarity, we have to clarify when anomalous diffusion appears, and what is the origin of the anomaly.

Latora *et al.* [10] discussed the relation between the process of relaxation to equilibrium and anomalous diffusion in a globally coupled rotator system, by comparing the time series of the temperature and of the mean squared displacement of the phases of the rotators. They showed that anomalous diffusion changes to a normal diffusion after a crossover time, and that the crossover time coincides with the time when the canonical temperature is reached. They also claim that anomalous diffusion occurs in the quasistationary states, which appear before the system goes towards equilibrium.

The crossover from anomalous to normal diffusion determines the time when the anomalous diffusion finishes. However, it is not clearly pointed out when the anomalous diffusion starts, and hence the study of the relation between the relaxation process and anomalous diffusion is still not complete. Moreover, in Ref. [10], the numerical calculations were performed by using only one type of initial condition, but different types of initial condition may change the conclusion [16].

*Electronic address: yyama@i.kyoto-u.ac.jp

In this paper, we study the globally coupled rotator system considered in Refs. [10,17], and we exhibit the relation between relaxation to equilibrium and anomalous diffusion with a different type of initial condition from the one used in Refs. [10,17]. Then we show that diffusion becomes anomalous if and only if the state is neither stationary nor quasistationary. In other words, diffusion is shown to be normal in quasistationary states, although a stretched exponential correlation function is present, contrary to previous claims that report power law type function [17]. Simple scaling laws of the correlation function imply that the result holds irrespective of degrees of freedom.

This paper is organized as follows. The model, initial condition, and observed quantities are described in Sec. II. In Sec. III, we study relaxation process, which we divide into three stages: quasi-stationary, relaxational, and equilibrium stages. Diffusion process in each stage is investigated in Sec. IV by using stretched exponential correlation functions of momenta. Dependence on degrees of freedom is also reported both in Secs. III and IV. Section V is devoted to summary.

II. MODEL, INITIAL CONDITION, AND OBSERVED QUANTITIES

The model considered in this paper has N classical and identical rotators confined to move on the unit circle, and the Hamiltonian is composed of a kinetic part and a potential part [1,2,5,10,17],

$$H=K+V=\sum_{j=1}^{N}\frac{p_j^2}{2}+\frac{1}{2N}\sum_{i,j=1}^{N}[1-\cos(\theta_i-\theta_j)]. \quad (1)$$

The N particles are globally coupled through the mean field defined as

$$\boldsymbol{M}=\frac{1}{N}\sum_{j=1}^{N}(\cos\theta_j,\sin\theta_j)=M(\cos\phi,\sin\phi), \quad (2)$$

where the modulus $M(0\leqslant M\leqslant 1)$ represents the magnetization of this system. We remark that the potential V and the kinetic energy K are related to the magnetization M as follows:

$$2V/N=1-M^2, \quad 2K/N=2U-1+M^2, \tag{3}$$

where U is the energy per particle, i.e., $U=E/N$, and E is the total energy. The free energy of this system has been obtained in the canonical ensemble [1,2,18], and it has been shown that system (1) has a second-order phase transition at the critical energy $U_c=0.75$. If the energy U is greater than the critical energy, the largest Lyapunov exponent goes to zero in the thermodynamic limit ($N\to\infty$) [19]. Then, all rotators freely rotate, and diffusion becomes ballistic. On the contrary, if U is small compared to U_c, all rotators are trapped in the potential well and no diffusion occurs. We are therefore interested in a value of the energy which is near but less than the critical energy in order to allow some particle diffusion. Hereafter, we set $U=0.69$ (a value studied also in Refs. [10,17,18]).

The canonical equations of motion for system (1) can be cast in a form that uses the mean field Eq. (2) as follows:

$$\frac{\mathrm{d}\theta_j}{\mathrm{d}t}=p_j, \quad \frac{\mathrm{d}p_j}{\mathrm{d}t}=-M(t)\sin(\theta_j-\phi(t)), \quad (j=1,\ldots,N). \tag{4}$$

We numerically integrate Eq. (4) by using fourth-order symplectic integrators [20,21]. The time slice of the integrator is set at $\Delta t=0.2$ or 0.4, and it suppresses the relative energy error down to $|\Delta E/E|<5\times10^{-7}$.

We have performed the integrations starting from $M(0)=0$. To prepare these initial conditions numerically, we set $q_j(0)=2\pi j/N$, and $p_j(0)$ is taken from a uniformly random distribution whose support is $[-\overline{p},\overline{p}]$, where the value $\overline{p}$ is chosen to get the energy density U. The total momentum $\Sigma_{j=1}^{N}p_j$ is an integral of the motion and we initially set it to zero. This initial state corresponds to a local entropy minimum [22], and to a stationary stable solution to the Vlasov-Poisson equation [2], although the system goes towards Gibbs equilibrium due to finite size effects [6]. With respect to the $M(0)=1$ initial condition chosen in Refs. [10,17], the one we choose has the advantage of being a quasistationary state from the start.

We numerically observe the time series of two quantities. One is for the relaxation process and the other is for the diffusion process.

To observe the relaxation process, we use the magnetization $M(t)$. Note that observing $M(t)$ corresponds to observing $2K(t)/N$ by using Eq. (3), and $2K(t)/N$ is the time series of the temperature, since the canonical average of $2K/N$ coincides with the canonical temperature.

To observe the diffusion process, we introduce the mean square displacement of phases $\sigma_\theta^2(t)$ defined as

$$\sigma_\theta^2(t)=\frac{1}{N}\sum_{j=1}^{N}[\theta_j(t)-\theta_j(0)]^2=\langle[\theta_j(t)-\theta_j(0)]^2\rangle_N. \tag{5}$$

The symbol $\langle\cdot\rangle_N$ represents the average over all the N rotators. The quantity $\sigma_\theta^2(t)$ typically scales as $\sigma_\theta^2(t)\sim t^\alpha$, and the diffusion is anomalous when $\alpha\neq1,2$, while it is normal when $\alpha=1$ and ballistic for $\alpha=2$. The quantity $\sigma_\theta^2(t)$ can be rewritten by using the correlation function of momenta $C_p(t;\tau)$ as

$$\sigma_\theta^2(t)=\int_0^t\mathrm{d}t_1\int_0^t\mathrm{d}t_2\ \langle p_j(t_1)p_j(t_2)\rangle_N =2\int_0^t\mathrm{d}s\int_0^{t-s}\mathrm{d}\tau\ C_p(s;\tau), \tag{6}$$

where $C_p(t;\tau)$ is defined as

$$C_p(t;\tau)=\langle p_j(t+\tau)p_j(\tau)\rangle_N. \tag{7}$$

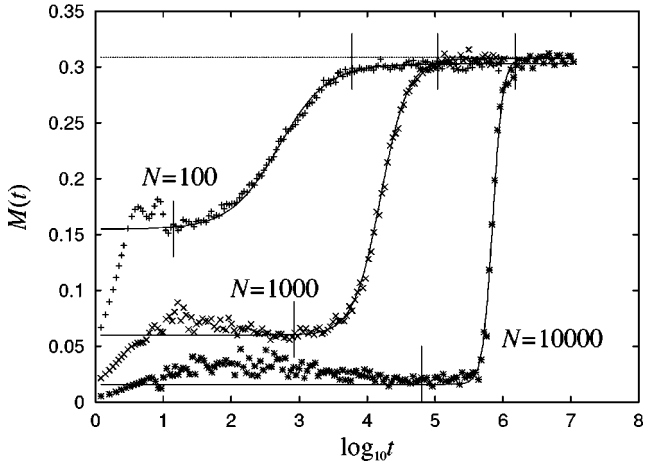

FIG. 1. Temporal evolutions of $M(t)$. $U=0.69$ and $N=100$, 1000, 10 000. The horizontal line represents the canonical equilibrium value of M. On each curve, two short vertical lines are marked. The first and the second ones are at the end of stages I and II, respectively. Solid curves are hyperbolic tangent functions (10).

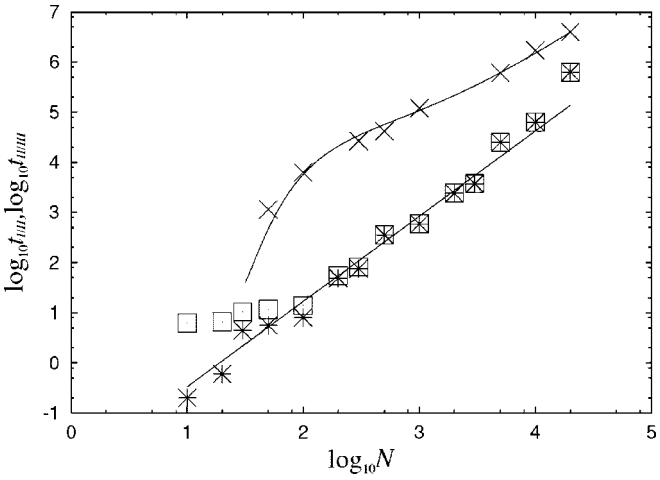

FIG. 2. Dependence on degrees of freedom of $t_{\mathrm{I/II}}$ (squares) and $t_{\mathrm{II/III}}$ (crosses). Stars represent $t_{\mathrm{I/II}}-6$. The lower straight line represents the power law $N^{1.7}/150$. The upper curve is a theoretical prediction of the boundary time $t_{\mathrm{II/III}}$ using Eqs. (11) and (12) with $M_{\mathrm{th}}=0.99M_{\mathrm{eq}}$.

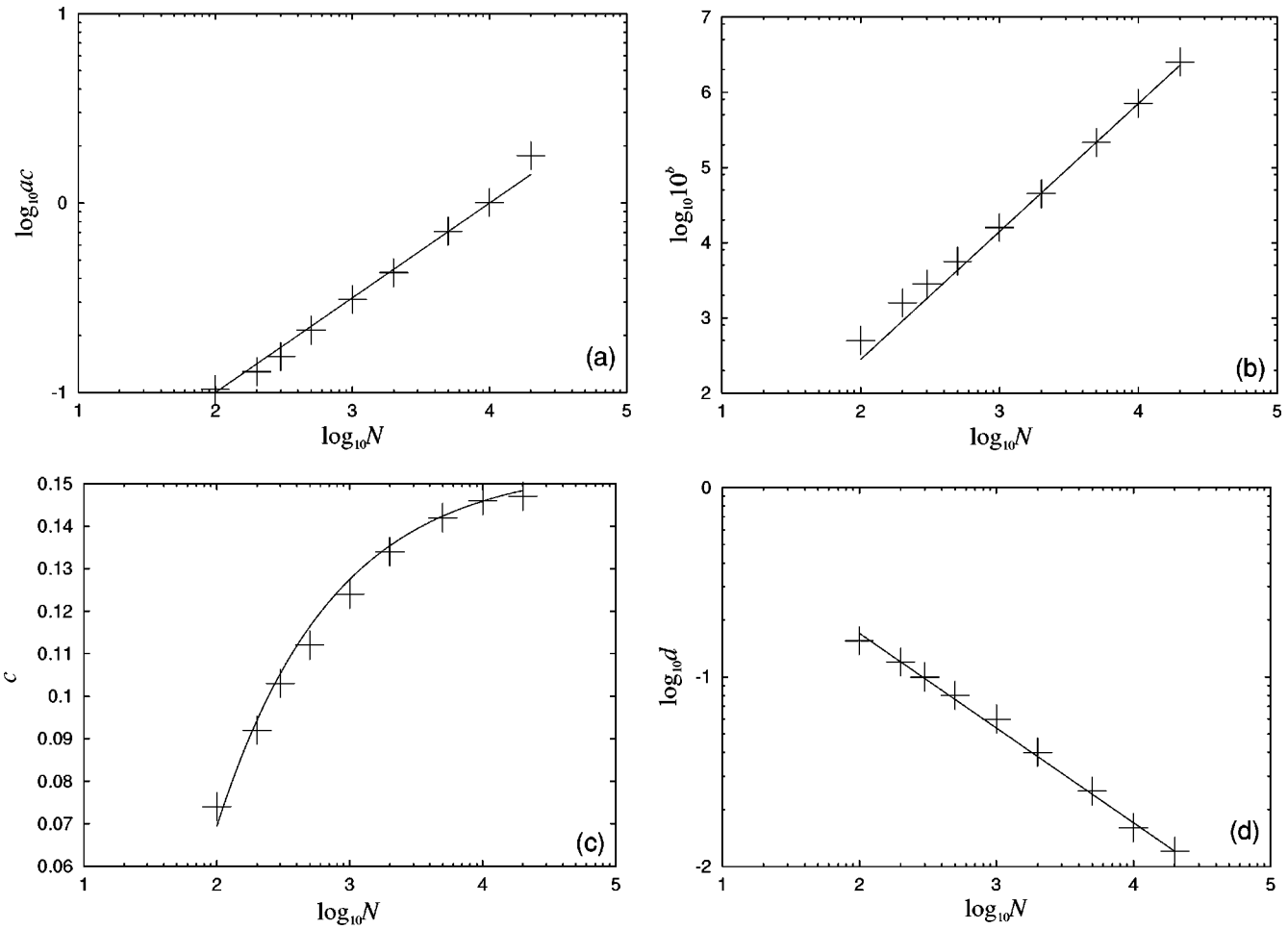

FIG. 3. Four parameters a, b,c, and d are reported as functions of degrees of freedom. (a) Log-log plot of ac. (b) Log-log plot of 10^b. (c) Liner-log plot of c. (d) Log-log plot of d. Solid curves are scaling functions described in Eq. (11).

Moreover, if the system is stationary and $C_p(t;\tau)$ does not depend on τ accordingly,

$$C_p(t;\tau)=C_p(t;0), \quad (\forall \quad \tau>0) \tag{8}$$

then Eq. (6) is simplified as

$$\sigma_\theta^2(t)=2\int_0^t (t-s)C_p(s;0)\ \mathrm{d}s. \tag{9}$$

III. RELAXATION PROCESS

Temporal evolutions of $M(t)$ are shown in Fig. 1. In order to suppress fluctuations, we have calculated averages over realizations. Throughout this paper, unless no comments appear, the number of realizations are $n=1000$, 100, and 8 for $N=100$, 1000, and 10 000, respectively. We divide the temporal evolutions into three stages, I, II, and III. In stage I, the value of magnetization is almost constant but smaller than the canonical value. After stage I, magnetization rapidly increases towards its equilibrium value M_{eq}, and we call this time interval stage II. Finally the system reaches equilibrium during stage III.

Let us define boundary times between stages I and II, $t_{\mathrm{I/II}}$, and between stages II and III, $t_{\mathrm{II/III}}$, as follows. The magnetization takes the local minimum at $t_{\min}$, and we adopt $t_{\mathrm{I/II}}=t_{\min}$. We define the other boundary time $t_{\mathrm{II/III}}$ as the first passage time which satisfies $M(t)=0.99M_{\mathrm{eq}}$. Values of the two boundary times are reported in Fig. 2 as functions of degrees of freedom. The local minimum time is proportional to $N^{1.7}$ for $N\geqslant 100$ with our initial condition $M(0)=0$, as with another initial condition $M(0)=1$ [23]. For small N, we cannot neglect the initial time region $t<6$ in which the level of $M(t)$ goes to $O(1/\sqrt{N})$ coming from the law of large numbers [see Fig. 3(d)], and hence the power law breaks. The power law recovers by subtracting the initial increasing time 6 from $t_{\mathrm{I/II}}$ as shown in Fig. 2, i.e., $t_{\mathrm{I/II}}-6\sim N^{1.7}$ ($N\geqslant 10$).

A theoretical prediction of $t_{\mathrm{II/III}}$, the upper curve in Fig. 2, is obtained by fitting the magnetization $M(t)$ as hyperbolic tangent function,

$$M(t)=\{1+\tanh[a(\log_{10}t-b)]\}\ \ c+d. \tag{10}$$

The parameter d represents the initial level of $M(t)$, and c the half width between initial and equilibrium levels of $M(t)$. The product ac is the slope at $\log_{10}t=b$, i.e., ac

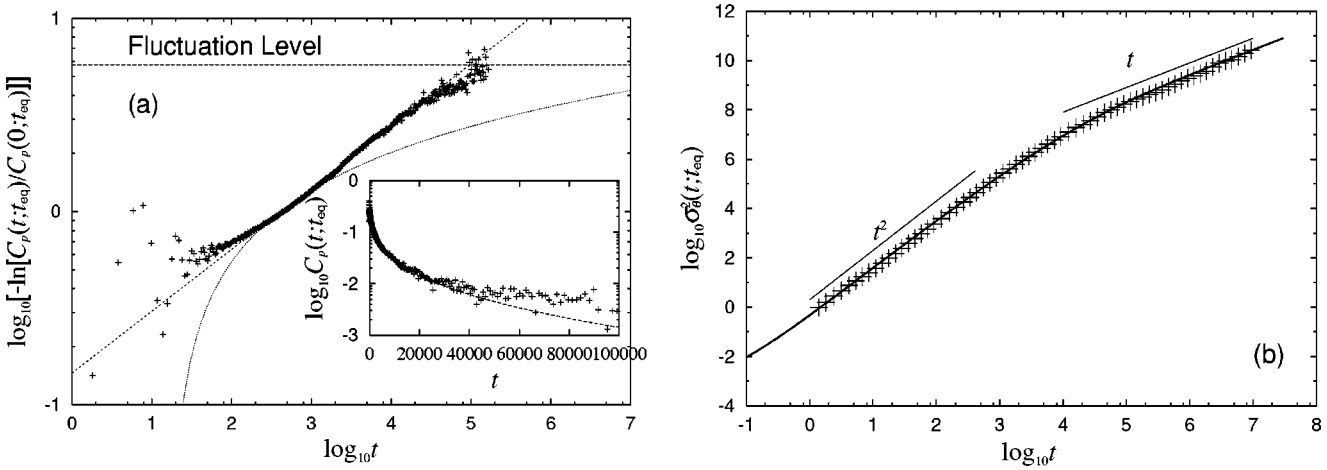

FIG. 4. (a) Double log-log plot of normalized correlation function $C_p(t;t_{\rm eq})/C_p(0;t_{\rm eq})$ at equilibrium with $t_{\rm eq}=2^{20}$, $N=1000$. We take an average over $n=100$ realizations. The straight line and the curve represent the stretched exponential function (16) and the power-type function $(t/410)^{-0.32}/e$, respectively. The upper horizontal line is fluctuation level $O(1/\sqrt{Nn})$. The inset shows a log-linear plot with the stretched exponential function. (b) Log-log plot of $\sigma^2_\theta(t;t_{\rm eq})$ with the approximate function produced by Eqs. (15) and (16).

$=\mathrm{d}M/\mathrm{d}(\log_{10}t)|_{\log_{10}t=b}$, and 10^b is the time scale. As shown in Fig. 3, these four parameters are fitted as

$$a(N)=\frac{\sqrt{N}}{100\ \ c(N)},\quad 10^{b(N)}=\frac{1}{9}N^{1.7},$$
$$c(N)=\frac{[M_{\rm eq}-d(N)]}{2},\quad d(N)=\frac{1.7}{\sqrt{N}}. \tag{11}$$

By using the scaling law Eq. (11), we can predict when $M(t)$ reaches a given threshold level, $M_{\rm th}$, as a function of N. Let $t_{\rm th}$ be the threshold time, which satisfies $M(t_{\rm th})=M_{\rm th}$, then $t_{\rm th}$ is expressed as

$$t_{\rm th}=10^b\left(\frac{M_{\rm th}-d}{M_{\rm eq}-M_{\rm th}}\right)^{(\ln 10)/2a}. \tag{12}$$

In Fig. 2, $t_{\rm th}$ is reported for $M_{\rm th}=0.99M_{\rm eq}$, and the prediction is in good agreement with numerical results. We remark that, roughly speaking, $t_{\rm II/III}$ is asymptotically proportional to $N^{1.7}$.

The system seems quasistationary in stage I. The existence of quasistationary states for sufficiently long time has been questioned in Ref. [23]. We will answer to the question by observing dependence on τ of the correlation function $C_p(t;\tau)$ in Sec. IV B.

IV. DIFFUSION PROCESS

As described in Eq. (6), the mean square displacement $\sigma^2_\theta(t)$ is obtained from correlation function of momenta $C_p(t;\tau)$, and hence we study diffusion process by observing the correlation function. We start from the simplest stage, stage III, because we may use the simple expression (9). Next, we progress to stage I, where we expect that the system is quasistationary, and that we may use Eq. (9) again. In nonstationary stage, stage II, we check whether diffusion is of a power type. Finally we investigate dependence on degrees of freedom for some important parameters.

A. Diffusion at equilibrium

Assuming the system has reached equilibrium at $t=t_{\rm eq}$, we observe $C_p(t;t_{\rm eq})$ and $\sigma^2_\theta(t;t_{\rm eq})$, where

$$\sigma^2_\theta(t;t_{\rm eq})=\langle[\theta_j(t+t_{\rm eq})-\theta_j(t_{\rm eq})]^2\rangle_N. \tag{13}$$

At equilibrium we may assume that the system is stationary,

$$C_p(t;t_{\rm eq}+\tau)=C_p(t;t_{\rm eq})\quad(\forall\ \ \tau>0), \tag{14}$$

and hence

$$\sigma^2_\theta(t;t_{\rm eq})=2\int_0^t(t-s)C_p(s;t_{\rm eq})\ \ \mathrm{d}s. \tag{15}$$

Now let us consider the correlation function for $N=1000$. We adopt $t_{\rm eq}=2^{20}\simeq 10^6$ which is long enough to reach equilibrium imaging from Fig. 1. The correlation function $C_p(t;t_{\rm eq})$ is reported in Fig. 4(a), and is well approximated by the stretched exponential function [24],

$$C_p(t;t_{\rm eq})=0.47\exp[-(t/410)^{0.32}], \tag{16}$$

rather than by a pure exponential [see the inset of Fig. 4(a) which is a log-linear plot of $C_p(t;t_{\rm eq})$].

We remark that a stretched exponential function $\exp[-x^\beta]$ with a small exponent $|\beta|\ll 1$ is indistinguishable from a power-type function in the region $|\beta\ln x|\ll 1$:

$$\exp[-x^\beta]=\exp[-\exp(\beta\ln x)]$$
$$\sim\exp[-1-\beta\ln x]$$
$$=x^{-\beta}/e.$$

However the fitting function (16) well agrees with the numerical result even around $|0.32\ln(t/410)|=1$, whose two solutions are $t\simeq 18$, 9330. We therefore adopt a stretched exponential function as an approximation of $C_p(t;t_{\rm eq})$.

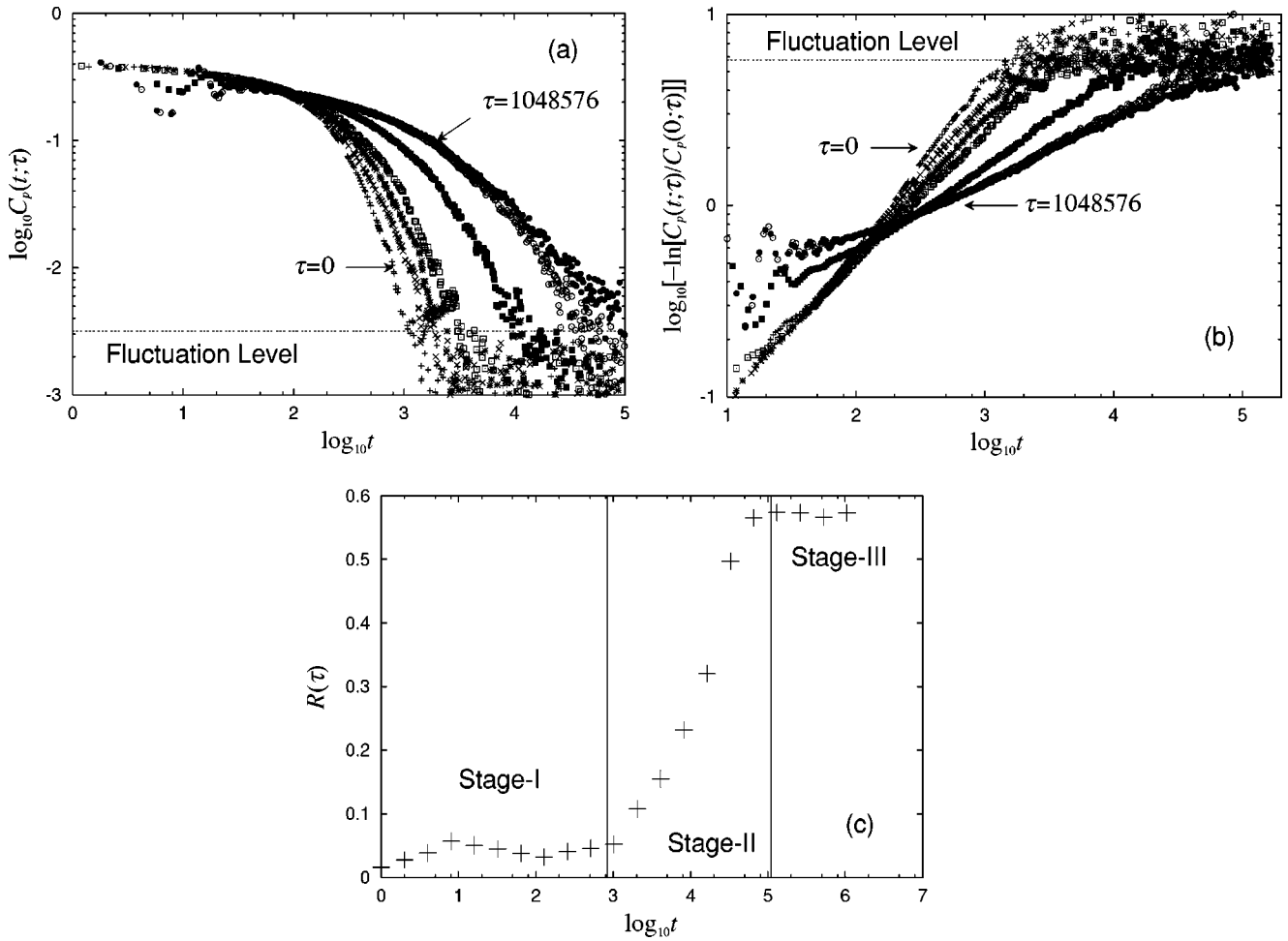

FIG. 5. Correlation function of momenta $C_p(t;\tau)$ for various values of $\tau=0$, 1024, 2048, 4096, 16 384, 65 536, and 1 048 576 from left to right. (a) Log-log plot. (b) Double log-log plot. (c) Relative error Eq. (18) of $C_p(t;\tau)$ from $C_p(t;0)$.

By using the fitting function (16) and Eq. (15), we numerically reproduce $\sigma_\theta^2(t;t_{\rm eq})$, and the reproduced curve well approximates the numerical result as shown in Fig. 4(b). Note that $\sigma_\theta^2(t;t_{\rm eq})$ is proportional to t^2 in the limit of $t\to 0$, since $C_p(s;t_{\rm eq})$ in Eq. (15) goes to the constant $C_p(0;t_{\rm eq})$. On the other hand, in the limit of $t\to\infty$, $\sigma_\theta^2(t;t_{\rm eq})$ is proportional to t, because both $C_p(s;t_{\rm eq})$ and $sC_p(s;t_{\rm eq})$ are almost zero in long time region, and hence their integrals become constants. The crossover from t^2 to t is also observed if we assume an exponential correlation function, and hence we conclude that diffusion at equilibrium is normal as expected although a stretched exponential is present.

B. Diffusion in quasistationary state

Except for stage III, we cannot expect stationarity to hold Eq. (8) any more. However, from the temporal evolutions of $M(t)$, Fig. 1, we may expect quasistationarity in stage I,

$$C_p(t;\tau)=C_p(t;0)+\epsilon(t;\tau), \tag{17}$$

where τ belongs to stage I and $\epsilon(t)$ is suitably small.

The correlation function $C_p(t;\tau)$ for various values of τ is reported in Figs. 5(a) and 5(b) for $N=1000$, and the relative error of correlation function defined as

$$R(\tau)=\max_t \frac{|\epsilon(t;\tau)|}{C_p(0;0)} \tag{18}$$

is also reported in Fig. 5(c) as a function of τ. The error $R(\tau)$ stays small up to the end of stage I, and hence we conclude that the system is quasistationary in stage I. We believe that the quasistationary states correspond to stationary stable states of the Vlasov equation [25]. We remark that $R(\tau)$ is constant in stage III again due to stationarity at equilibrium.

It seems natural that we regard $C_p(t;\tau)$ as a series of stretched exponential functions of t rather than power-type functions, since this function fits $C_p(t;\tau)$ in more than two decades of time (power law fits of the correlation functions hold in one decade). Moreover, at equilibrium, $C_p(t;t_{\rm eq})$ is also a stretched exponential rather than a pure exponential, as shown in Fig. 4.

In the quasistationary region, stage I, the mean square displacement $\sigma_\theta^2(t)$ can be derived by the correlation function $C_p(t;0)$, which is reported in Fig. 6 for $N=100$, 1000, and 10 000. We approximate $C_p(t;0)$ by a stretched exponential function as

$$N=100: \quad C_p(t;0)=0.38\exp[-(t/20)^{0.68}],$$

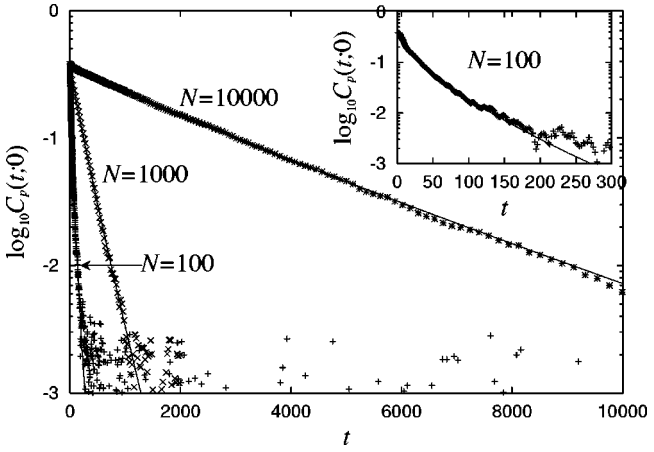

FIG. 6. Correlation function of momenta at $\tau=0$, i.e., $C_p(t;0)$. The inset is magnification of the horizontal axis around $t=0$ for $N=100$. These numerical results are approximated by solid curves which are stretched exponential functions (19).

$$N=1000: \quad C_p(t;0)=0.38\exp[-(t/180)^{0.91}],$$

$$N=10\,000: \quad C_p(t;0)=0.38\exp[-(t/2200)^{0.90}]. \quad (19)$$

The prefactor 0.38 comes from $C_p(0;0)=2K(0)/N$.

Using the approximate functions (19) and Eq. (9), we are able to reproduce $\sigma_\theta^2(t)$, as shown in Fig. 7. The approximation is good in stage I, i.e., in the quasistationary time region, irrespective of the value of N. Consequently, there is no anomaly in diffusion in stage I, since the diffusion is explained by stretched exponential correlation function.

C. Diffusion in nonstationary state

After the quasistationary region, diffusion becomes anomalous, which is faster than normal diffusion, in stage II. If we fit $\sigma_\theta^2(t)$ by a power-type function t^α in stage II, the exponent α is estimated as 1.54, 1.59, and 1.74 for $N=100$, 1000, and 10 000, respectively. The values of exponent tend to increase as N increases as reported for the system having the so-called two-dimensional egg-crate potential [3]. On the other hand, the duration in which diffusion is anomalous becomes shorter and shorter in logarithmic time scale as N increases, in accordance with the sharper change of $M(t)$. Moreover, σ_θ^2/t^α is not constant, but has a wave in stage II (see Fig. 8). Hence we guess that the anomaly in diffusion is not anomalous diffusion taking a power-type function but a transient anomaly due to nonstationarity of stage II.

Let us proceed to investigate the origin of anomaly in diffusion. We focus on the behavior for $N=1000$. The mean square displacement $\sigma_\theta^2(t)$ is perfectly determined by the correlation function $C_p(t;\tau)$ using Eq. (6), once we assume that $C_p(t;\tau)$ is a series of stretched exponential functions. We introduce three parameters, $C_p(0;\tau)$, $t_{\rm corr}(\tau)$, and $\beta(\tau)$, to describe the stretched exponential function as

$$C_p(t;\tau)=C_p(0;\tau)\exp[-\{t/t_{\rm corr}(\tau)\}^{\beta(\tau)}]. \quad (20)$$

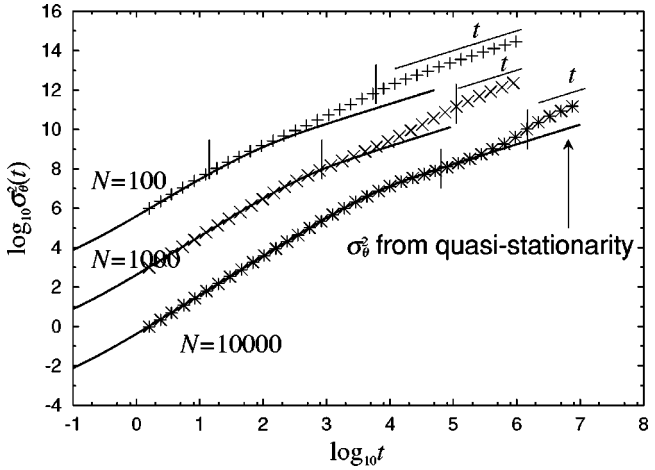

FIG. 7. Time series of the mean square displacement of the phases $\sigma_\theta^2(t)$. $N=100$, 1000, and 10 000 from top to bottom. The vertical axis is the original scale only for $N=10\,000$, and is multiplied by 10^3 and 10^6 for $N=1000$ and 100, respectively, just for a graphical reason. In stage I where the system is quasistationary, the numerical results are approximated by solid curves which are obtained from Eq. (9) using functions (19). After the system reaches equilibrium, diffusion becomes normal. Anomaly in diffusion is observed only in stage II. The two short vertical lines on each curve show the end of stages I and II, which correspond to those found in Fig. 1.

We investigate which of the three parameters is the most important to yield anomaly in diffusion.

The strategy is as follows. We reproduce $d\sigma_\theta^2(t)/dt$ by using the three parameters and the formula

$$\frac{d\sigma_\theta^2}{dt}(t)=2\int_0^t d\tau\ C_p(0;\tau)\exp[-\{(t-\tau)/t_{\rm corr}(\tau)\}^{\beta(\tau)}]. \quad (21)$$

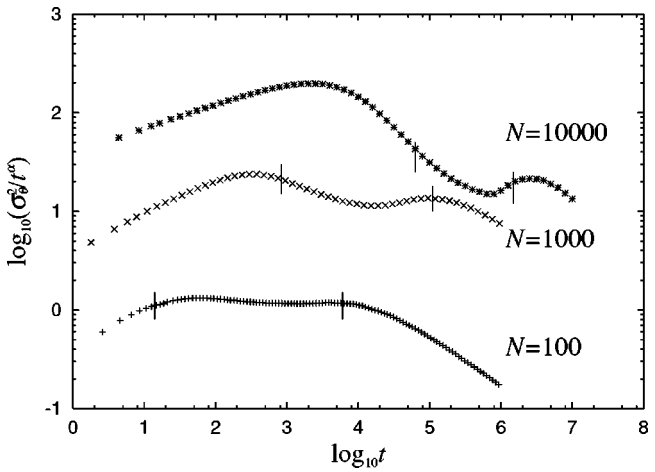

FIG. 8. Log-log plot of $\sigma_\theta^2(t)/t^\alpha$. The exponent α is estimated as 1.54, 1.59, and 1.74 for $N=100$, 1000, and 10 000, respectively. The two short vertical lines on each curve show the end of stages I and II. In stage II, σ_θ^2/t^α is not constant. The vertical axis is the original scale only for $N=100$, and is multiplied by 10 and 100 for $N=1000$ and $N=10\,000$, respectively for a graphical reason.

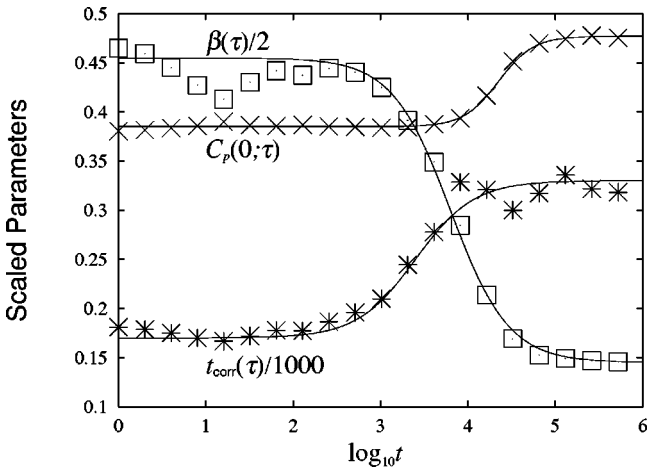

FIG. 9. The three parameters $C_p(0;\tau)$, $t_{\rm corr}(\tau)$, and $\beta(\tau)$ as functions of τ. The latter two parameters $t_{\rm corr}(\tau)$ and $\beta(\tau)$ are multiplied by 1/1000 and 1/2, respectively, for a graphical reason. Solid curves are hyperbolic tangent functions described in Eq. (22).

We consider the first derivative of σ_θ^2 instead of σ_θ^2 itself, because the former requires only single integration while the latter requires double integrations (6). We first omit the dependence on τ of the parameter $C_p(0;\tau)$ and fix it to a constant value to observe how it affects the anomaly in diffusion. We then fix the two other parameters $t_{\rm corr}(\tau)$ and $\beta(\tau)$ to determine their effect on the mean square displacement.

From the numerical results of $C_p(t;\tau)$, Fig. 5(b), we determine the values of three parameters $C_p(0;\tau)$, $t_{\rm corr}(\tau)$, and $\beta(\tau)$ at some value of τ by using the least square method. The discrete values of the parameters are not enough to reproduce $d\sigma_\theta^2(t)/dt$ accurately, and then we approximate the parameters by hyperbolic tangent functions as follows:

$$C_p(0;\tau)=0.046\ [1+\tanh(2.5(\log_{10}\tau-4.35))]+0.385,$$

$$t_{\rm corr}(\tau)=80\ [1+\tanh(1.5(\log_{10}\tau-3.4))]+170,$$

$$\beta(\tau)=0.31\ [1+\tanh(1.5(\log_{10}\tau-3.8))]+0.29. \quad (22)$$

The hyperbolic tangent functions are in good agreement with numerical results, as shown in Fig. 9. To confirm the validity of the approximation, we reproduced $\mathrm{d}\sigma_\theta^2/\mathrm{d}t$ using Eqs. (21) and (22), and the reproduced one is in good agreement with numerical results, as shown in Fig. 10(a).

If we fix $C_p(0;\tau)$ at its middle value 0.431 we find that the dependence on τ of $C_p(0;\tau)$ does not affect significantly $\mathrm{d}\sigma_\theta^2/\mathrm{d}t$, as shown in Fig. 10(b). By fixing $t_{\rm corr}(\tau)$ at its middle value 250 we obtain the same conclusion for $t_{\rm corr}(\tau)$ as for $C_p(0;\tau)$, particularly in stage II [see Fig. 10(c)]. On the contrary, if we fix $\beta(\tau)$ at 0.6 or 0.9, we observe no anomaly in diffusion as shown in Fig. 10(d), because $\mathrm{d}\sigma_\theta^2(t)/\mathrm{d}t$ is proportional to t and is constant in short and long time regions, respectively, and the same behavior is obtained at equilibrium [see Fig. 4(b)]. Consequently, among the three parameters, $\beta(\tau)$ plays a crucial role to produce anomaly in diffusion.

D. Dependence on degrees of freedom

In stage I (and III), we fit $C_p(t;0)$ [resp. $C_p(t;t_{\rm eq})$] by a stretched exponential function, which has three parameters: $C_p(0;0)$, $t_{\rm corr}(0)$, and $\beta(0)$ [resp. $C_p(0;t_{\rm eq})$, $t_{\rm corr}(t_{\rm eq})$, and $\beta(t_{\rm eq})$]. In order to obtain scaling laws for the parameters, we show them as functions of degrees of freedom N. The parameters $C_p(0;0)$ and $C_p(0;t_{\rm eq})$ represent temperature at $t=0$ and at equilibrium, respectively, and hence they do not depend on N. We therefore focus on the other four parameters, $t_{\rm corr}(0)$, $\beta(0)$, $t_{\rm corr}(t_{\rm eq})$, and $\beta(t_{\rm eq})$. The correlation functions, $C_p(t;0)$ and $C_p(t;t_{\rm eq})$, are shown in Fig. 11, and values of the four parameters are reported as functions of N in Fig. 12.

For large N, $N\geqslant 200$, the correlation times are proportional to N, that is, $t_{\rm corr}(0)=N/5$ and $t_{\rm corr}(t_{\rm eq})=N/2$, and the stretching exponents $\beta(0)$ and $\beta(t_{\rm eq})$ are almost constants. We expect that these scaling laws for the four quantities are kept even in the thermodynamic limit, although they break for small N, where $t_{\rm corr}(0)$ is larger than $N/5$ and $\beta(0)$ is smaller than the constant. The duration of stage I, $t_{\rm I/II}$, is around 23 for $N=100$, and hence $t_{\rm corr}(0)$ and $\beta(0)$ are estimated mainly not in stage I but in stage II from Fig. 11(a). In stage II, $t_{\rm corr}(\tau)$ and $\beta(\tau)$ are increasing and decreasing functions of τ, respectively (see Fig. 9), and hence $t_{\rm corr}(0)$ and $\beta(0)$ are larger and smaller than expected values, respectively.

V. SUMMARY

As a summary, we have investigated the relation between relaxation and diffusion in a Hamiltonian system with long-range interactions. The relaxation process is divided into three stages: quasistationary, relaxational, and equilibrium. We showed that diffusion becomes anomalous only in the second nonstationary stage, where magnetization is increasing and goes towards to the canonical value. The result mentioned above does not depend on the number of degrees of freedom, at least from $N=100$ to 10 000.

The interval where the anomaly in diffusion appears becomes shorter and shorter in logarithmic time scale as N increase corresponding to a sharper change of magnetization. Moreover, a detailed investigation exhibits the absence of power-type diffusion even in the nonstationary stage. We guess that anomaly in diffusion is a transient anomaly due to nonstationarity.

Diffusion is obtained by integrating the correlation function of momenta $C_p(t;\tau)$ and the correlation function is approximated by a series of stretched exponential functions $C_p(t;\tau)=C_p(0;\tau)\ \exp[-(t/t_{\rm corr}(\tau))^{\beta(\tau)}]$. Among the three parameters, $C_p(0;\tau)$, $t_{\rm corr}(\tau)$, and $\beta(\tau)$, the stretching exponent $\beta(\tau)$ plays a crucial role to yield anomaly in diffusion. If we assume that $\beta(\tau)$ is a constant, we never observe anomaly in diffusion. This result is consistent with the fact that anomaly in diffusion does not appear in (quasi)stationary state, because correlation function $C_p(t;\tau)$ and $\beta(\tau)$, accordingly, are almost invariant with respect to τ.

We also investigated scaling laws concerning degrees of freedom N. The duration of quasistationary stage is propor-

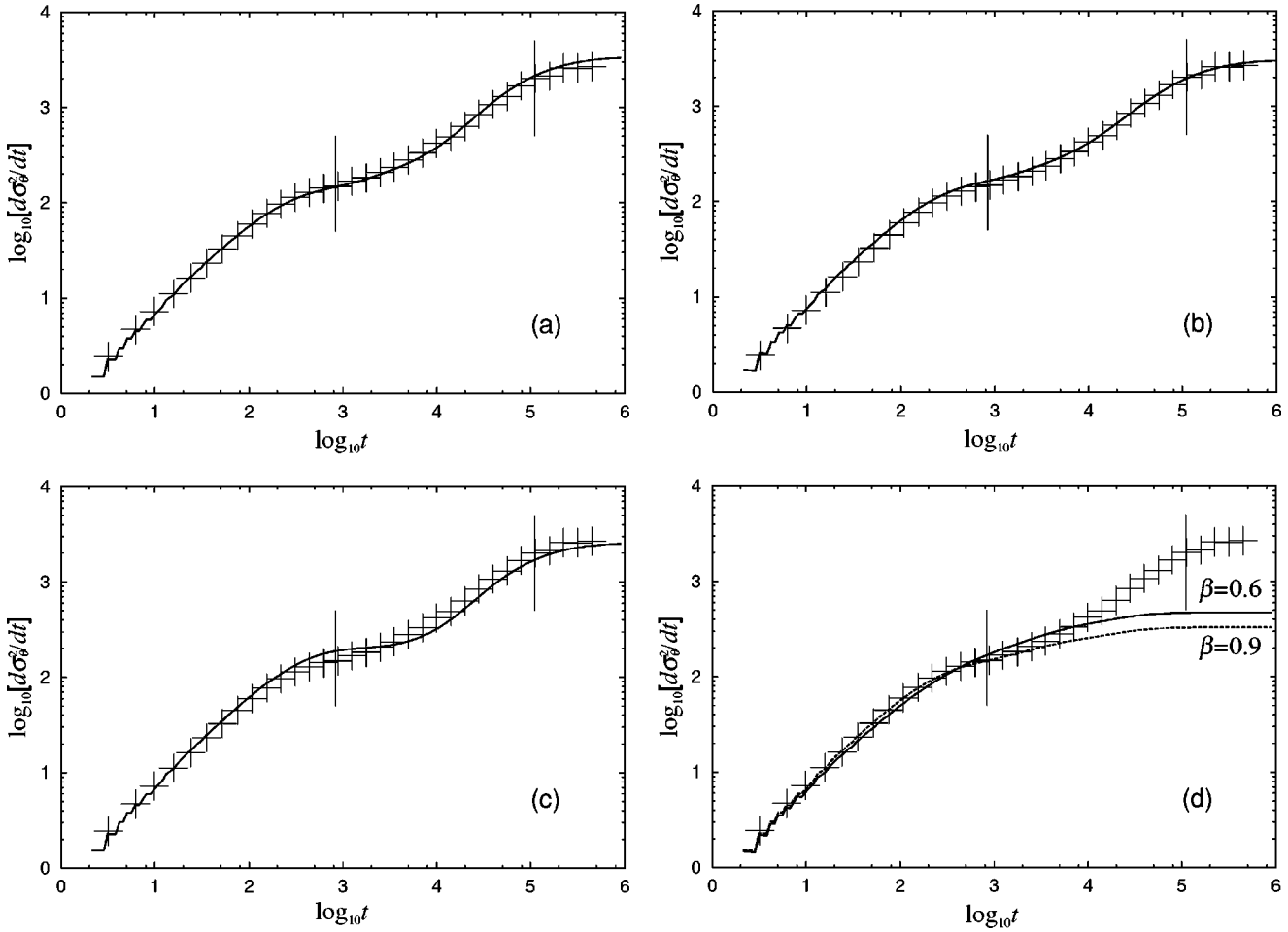

FIG. 10. Time derivative of the mean square displacement , $d\sigma_\theta^2(t)/dt$. (a) Numerical results (crosses) and reproduced one (solid curve) using Eq. (21) and the approximate functions of the three parameters in Eq. (22). In (b), (c), and (d), $C_p(0;\tau)$, $t_{\rm corr}(\tau)$, and $\beta(\tau)$ are kept constant, respectively. In (d), two constants for $\beta(\tau)$ have been tested. Solid and dashed curves represent $\beta=0.6$ and 0.9, respectively. The short vertical lines mark the end of stages I and II.

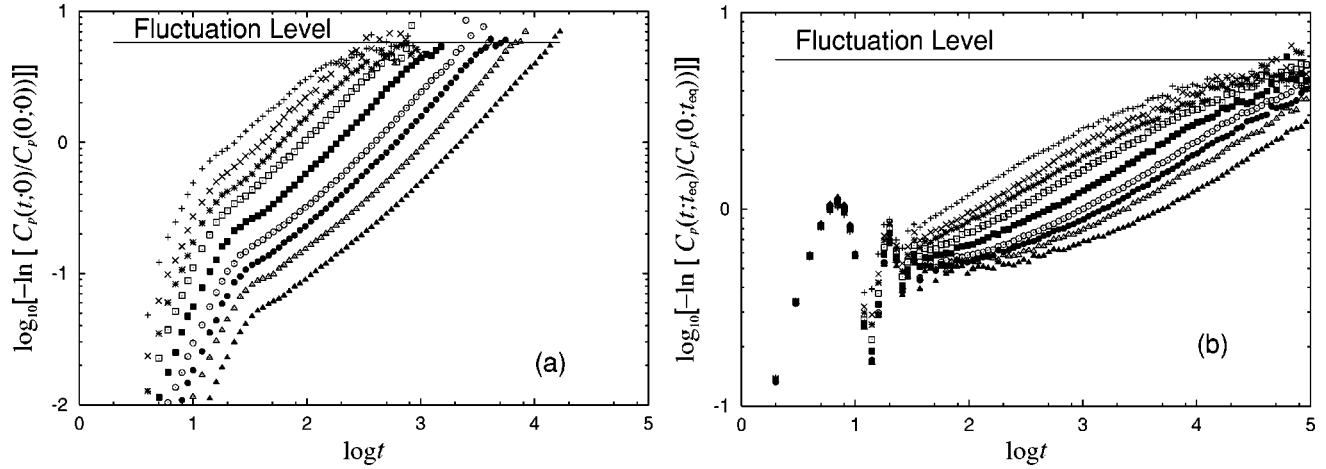

FIG. 11. Double log-log plots of correlation functions for various values of degrees of freedom N. (a) $C_p(t;0)$ (stage I). (b) $C_p(t;t_{\rm eq})$ (stage III). In both (a) and (b), $N=100(1000)$, 200(500), 300(300), 500(200), 1000(100), 2000(100), 3000(50), 5000(10), and 10 000(10) from top to bottom, where the inside of parentheses represent numbers of realizations for $C_p(t;t_{\rm eq})$. For $C_p(t;0)$, the number is 1000 for $N=1000$ and is 100 for the others.

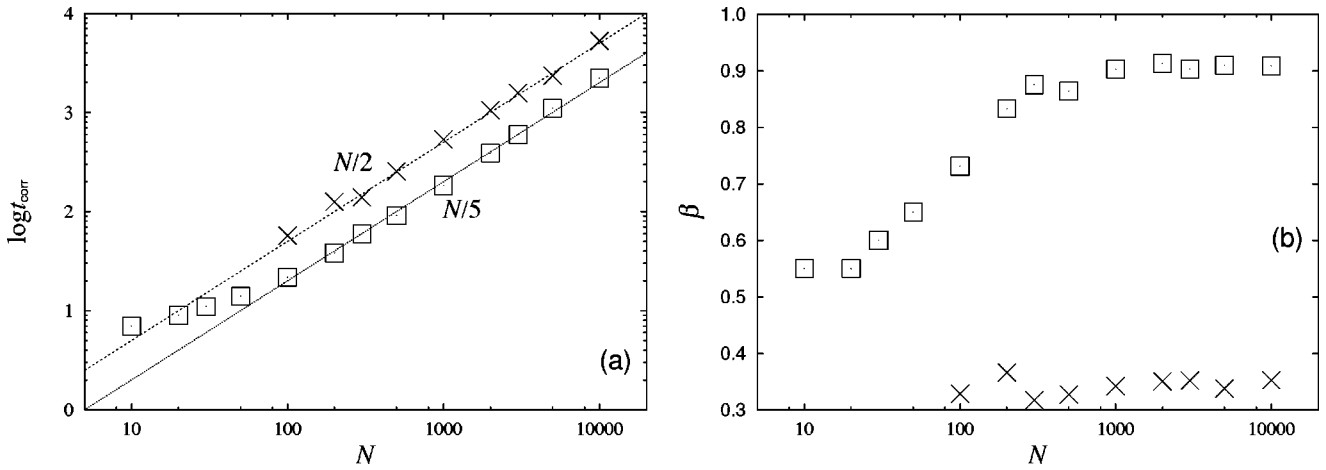

FIG. 12. Two parameters of correlation function as functions of degrees of freedom, $t_{corr}(N)$ (a) and $\beta(N)$ (b). In both (a) and (b), squares ($\times$) represent values of the parameters for $C_p(t;0)$ (stage I) and crosses ($\times$) for $C_p(t;t_{eq})$ (stage III).

tional to $N^{1.7}$, and relaxation time, at which the system reaches at equilibrium, is also proportional to $N^{1.7}$ asymptotically although some corrections must be added. In both quasistationary and equilibrium stages, t_{corr} is proportional to N and β is almost constant. These simple scaling laws imply that fitting by stretched exponential functions is valid irrespective of degrees of freedom.

We have not understood the theoretical reason of the appearance of a stretched exponential function. If we assume that several time scales with exponential correlation function, $\exp(-t/t_{corr})$, are present, and we assume probability distribution function of t_{corr}, $P(t_{corr})$, then we obtain a stretched exponential function $\int P(t_{corr})\exp(-t/t_{corr})dt_{corr}$ by choosing suitable forms for $P(t_{corr})$ [26,27]. In our model, $P(t_{corr})$ corresponds to the distribution of time scales of individual rotators. The investigation of the macrovariable $C(t;\tau)$ in relation with the microvariables of the individual particle correlation functions will be a subject of future work.

ACKNOWLEDGMENTS

I thank Stefano Ruffo for a careful reading of the manuscript and useful comments. I acknowledge valuable discussions with Alessandro Torcini, Freddy Bouchet, and Julien Barré.

[1] S. Ruffo, in *Transport and Plasma Physics*, edited by S. Benkadda *et al.* (World Scientific, Singapore, 1994), p. 114.
[2] M. Antoni and S. Ruffo, Phys. Rev. E **52**, 2361 (1995).
[3] A. Torcini and M. Antoni, Phys. Rev. E **59**, 2746 (1999).
[4] T. Tsuchiya, N. Gouda, and T. Konishi, Phys. Rev. E **53**, 2210 (1996).
[5] Y.Y. Yamaguchi, Prog. Theor. Phys. **95**, 717 (1996).
[6] V. Latora, A. Rapisarda, and C. Tsallis, Physica A **305**, 129 (2002); Phys. Rev. E **64**, 056134 (2001).
[7] T. Geisel, J. Nierwetberg, and A. Zacherl, Phys. Rev. Lett. **54**, 616 (1985).
[8] J. Klafter and G. Zumofen, Phys. Rev. E **49**, 4873 (1994).
[9] V. Latora, A. Rapisarda, and S. Ruffo, Phys. Rev. Lett. **80**, 692 (1998).
[10] V. Latora, A. Rapisarda, and S. Ruffo, Phys. Rev. Lett. **83**, 2104 (1999).
[11] K. Kaneko and T. Konishi, Phys. Rev. A **40**, 6130 (1989).
[12] T.H. Solomon, E.R. Weeks, and H.L. Swinney, Phys. Rev. Lett. **71**, 3975 (1993).
[13] J.D. Meiss and E. Ott, Phys. Rev. Lett. **55**, 2741 (1985); Physica D **13**, 395 (1984).
[14] G.M. Zaslavsky, D. Stevens, and H. Weitzner, Phys. Rev. E **48**, 1683 (1993).
[15] T. Geisel, in *Lévy Flights and Related Topics in Physics*, edited by M. F. Schlesinger *et al.* (Springer-Verlag, New York, 1995), p. 153, see also references therein.
[16] H. Koyama and T. Konishi, Phys. Lett. A **279**, 226 (2001).
[17] M.A. Montemurro, F. Tamarit, and C. Anteneodo, Phys. Rev. E **67**, 031106 (2003).
[18] V. Latora, A. Rapisarda, and S. Ruffo, Physica D **131**, 38 (1999).
[19] M.-C. Firpo, Phys. Rev. E **57**, 6599 (1998).
[20] H. Yoshida, Phys. Lett. A **150**, 262 (1990); Celest. Mech. Dyn. Astron. **56**, 27 (1993).
[21] R.I. McLachlan and P. Atela, Nonlinearity **5**, 541 (1992).
[22] M. Antoni, H. Hinrichsen, and S. Ruffo, Chaos, Solitons Fractals **13**, 393 (2002).
[23] D.H. Zanette and M.A. Montemurro, Phys. Rev. E **67**, 031105 (2003).
[24] J.C. Phillips, Rep. Prog. Phys. **59**, 1133 (1996).
[25] Y. Y. Yamaguchi, J. Barré, F. Bouchet, T. Dauxiois, and S. Ruffo (unpublished).
[26] R.G. Palmer, D.L. Stein, E. Abrahams, and P.W. Anderson, Phys. Rev. Lett. **53**, 958 (1984).
[27] R.A. Pelcovits and D. Mukamel, Phys. Rev. B **28**, 5374 (1983).